HGG Advances

ARTICLE

TMEM218 dysfunction causes ciliopathies, including Joubert and Meckel syndromes

Julie C. Van De Weghe,[1] Jessica L. Giordano,[2] Inge B. Mathijssen,[3] Majid Mojarrad,[4,5,6] Dorien Lugtenberg,[7] Caitlin V. Miller,[1] Jennifer C. Dempsey,[1] Mahsa Sadat Asl Mohajeri,[4] Elizabeth van Leeuwen,[8] Eva Pajkrt,[8] Caroline C.W. Klaver,[9] Henry Houlden,[10] Atieh Eslahi,[4,11] Aoife M. Waters,[12] University of Washington Center for Mendelian Genomics,[13] Michael J. Bamshad,[1,13,14] Deborah A. Nickerson,[13,14] Vimla S. Aggarwal,[15] Bert B.A. de Vries,[7] Reza Maroofian,[10] and Dan Doherty[1,16,17,*]

Summary

The Joubert-Meckel syndrome spectrum is a continuum of recessive ciliopathy conditions caused by primary cilium dysfunction. The primary cilium is a microtubule-based, antenna-like organelle that projects from the surface of most human cell types, allowing them to respond to extracellular signals. The cilium is partitioned from the cell body by the transition zone, a known hotspot for ciliopathy-related proteins. Despite years of Joubert syndrome (JBTS) gene discovery, the genetic cause cannot be identified in up to 30% of individuals with JBTS, depending on the cohort, sequencing method, and criteria for pathogenic variants. Using exome and targeted sequencing of 655 families with JBTS, we identified three individuals from two families harboring biallelic, rare, predicted-deleterious missense *TMEM218* variants. Via MatchMaker Exchange, we identified biallelic *TMEM218* variants in four additional families with ciliopathy phenotypes. Of note, four of the six families carry missense variants affecting the same highly conserved amino acid position 115. Clinical features included the molar tooth sign (N = 2), occipital encephalocele (N = 5, all fetuses), retinal dystrophy (N = 4, all living individuals), polycystic kidneys (N = 2), and polydactyly (N = 2), without liver involvement. Combined with existing functional data linking TMEM218 to ciliary transition zone function, our human genetic data make a strong case for TMEM218 dysfunction as a cause of ciliopathy phenotypes including JBTS with retinal dystrophy and Meckel syndrome. Identifying all genetic causes of the Joubert-Meckel spectrum enables diagnostic testing, prognostic and recurrence risk counseling, and medical monitoring, as well as work to delineate the underlying biological mechanisms and identify targets for future therapies.

Introduction

Joubert syndrome (JBTS [MIM: PS213300]) is a recessive, neurodevelopmental disorder defined by the appearance of the "molar tooth sign" on axial MRI. The prevalence of JBTS is estimated to be ~1/100,000 individuals.[1] Since the initial description in 1969 by Marie Joubert,[2] >38 genes have been linked to JBTS.[3] The pathognomonic brain imaging feature, the molar tooth sign, consists of cerebellar vermis hypoplasia and thick, misoriented superior cerebellar peduncles with a deep interpeduncular fossa. People with JBTS often have some degree of cognitive impairment, along with ataxia, apnea/tachypnea, abnormal eye movements, and hypotonia. Variable features include retinal degeneration, cystic kidneys, hepatic fibrosis, and polydactyly. JBTS overlaps with Meckel syndrome (MIM: PS249000), typically defined by a variable combination of occipital encephalocele, polydactyly, polycystic kidneys, congenital liver fibrosis, and demise during pregnancy or the neonatal period. To date, approximately one-third of JBTS-associated genes have also been linked to Meckel syndrome. Based on the genetic and phenotypic overlap, Joubert and Meckel syndromes likely represent the milder and more severe ends, respectively, of a ciliopathy spectrum.

Large cohorts of families with ciliopathies, coupled with powerful advances in genomics and data-sharing, have facilitated the identification of more than 38 genes associated with JBTS over the past decade. Despite this progress, 5%–30% (depending on the cohort) of individuals with JBTS still lack a genetic etiology.[4–6] Based on functional work in model

[1]Department of Pediatrics, University of Washington, Seattle, WA 98195, USA; [2]Department of OB/GYN, Columbia University Vagelos College of Physicians and Surgeons, New York, NY 10032, USA; [3]Department of Clinical Genetics, Amsterdam UMC, University of Amsterdam, Amsterdam, the Netherlands; [4]Department of Medical Genetics, Faculty of Medicine, Mashhad University of Medical Sciences, Mashhad, Iran; [5]Genetic Research Center, Faculty of Medicine, Mashhad University of Medical Sciences, Mashhad, Iran; [6]Genetic Center of Khorasan Razavi, Mashhad, Iran; [7]Department of Human Genetics, Radboud University Medical Center, Nijmegen, the Netherlands; [8]Department of Obstetrics and Gynecology, Amsterdam UMC, University of Amsterdam, Amsterdam, the Netherlands; [9]Department of Ophthalmology, Radboud University Medical Center, Nijmegen, the Netherlands; [10]Department of Neuromuscular Disorders, University College London Institute of Neurology, Queen Square, London WC1N 3BG, UK; [11]Student Research Committee, Faculty of Medicine, Mashhad University of Medical Sciences, Mashhad, Iran; [12]Great Ormond Street Hospital NHS Foundation Trust, London WC1N 1LE, UK; [13]University of Washington Center for Mendelian Genomics, Seattle, WA 98195, USA; [14]Department of Genome Sciences, University of Washington, Seattle, WA 98195, USA; [15]Department of Pathology and Cell Biology, Columbia University Vagelos College of Physicians and Surgeons, New York, NY, 10032 USA; [16]Center for Integrative Brain Research, Seattle Children's Research Institute, Seattle, WA 98101 USA
[17]Twitter: @Dohertylab
*Correspondence: ddoher@uw.edu
https://doi.org/10.1016/j.xhgg.2020.100016.

organisms, both Vogel et al.[7] and Li et al.[8] predicted that TMEM218 dysfunction could cause human ciliopathy phenotypes. Herein, we report discovery of biallelic pathogenic variants in *TMEM218* in 10 individuals from 6 families affected by either Joubert or Meckel syndrome.

Material and methods

Subject ascertainment and phenotypic data

All families were enrolled under approved human subjects research protocols at the University of Washington (UW), Columbia University Medical Center (CUMC), Radboud University Medical Center (RUMC), University College London (UCL), Amsterdam University Medical Center (AUMC), and Mashhad University of Medical Sciences, except for GM07817, which is a fibroblast cell line from a fetus diagnosed with Meckel syndrome of unknown genetic cause available through the Coriell cell repository. Clinical data were obtained by direct examination of participants, review of medical records, and structured questionnaires.

Variant identification

UW samples: Individuals affected by JBTS were previously screened using a molecular inversion probes (MIPs) targeted capture,[4,9] covering AHI1 (MIM: 608894), ARL13B (MIM: 608922), ARMC9 (MIM:617612), B9D1 (MIM: 614144), B9D2 (MIM: 611951), C2CD3 (MIM: 615944), CPLANE1 (MIM: 614571), CC2D2A (MIM: 612013), CEP290 (MIM: 61042), CEP41 (MIM: 610523), CSPP1 (MIM: 611654), IFT172 (MIM: 607386), INPP5E (MIM: 613037), KIF7 (MIM: 611254), MKS1 (MIM: 609883), NPHP1 (MIM: 607100), OFD1 (MIM: 300170), RPGRIP1L (MIM: 610937), TCTN1 (MIM: 609863), TCTN2 (MIM: 613846), TCTN3 (MIM: 613847), TMEM138 (MIM: 614459), TMEM216 (MIM: 613277), TMEM231 (MIM: 614949), TMEM237 (MIM: 614423), TMEM67 (MIM: 609884), TOGARAM1 (MIM: 617618), TTC21B (MIM: 612014), and ZNF423 (MIM: 604557).

In samples without biallelic rare, predicted-deleterious variants (RDVs), exome sequencing was performed as previously described[10] using Roche Nimblegen SeqCap EZ Human Exome Library v2.0 capture probes (36.5 Mb of coding exons) and paired-end 50 bp reads on an Illumina HiSeq sequencer. In accordance with the Genome Analysis ToolKit's (GATK) best practices, we mapped sequence reads to the human reference genome (hg19) using the Burrows-Wheeler Aligner (BWA, v.0.7.8), removed duplicate reads (PicardMarkDuplicates v.1.113), and performed indel realignment (GATK IndelRealigner v.3.1) and base-quality recalibration (GATK TableRecalibration v.3.1). We called variants using the GATK UnifiedGenotyper and flagged with VariantFiltration to mark potential false positives that did not pass the following filters: Heterozygous Allele Balance (ABHet) > 0.75, Quality by Depth > 5.0, Quality (QUAL) > 50.0, Homopolymer Run (Hrun) < 4.0, and low depth ($< 8\times$). We used SeattleSeq for variant annotation and the Combined Annotation Dependent Depletion (CADD) score to determine deleteriousness of identified missense variants.[11] Based on CADD score data for causal variants in other JBTS-associated genes, we used a CADD score cutoff of 15 to define deleterious variants.[4]

CUMC family: Research trio analysis was performed as previously described.[12] In brief, DNA samples were exome sequenced by the Institute for Genomic Medicine, Columbia University Medical Center. Whole exome sequencing (WES) was performed with the KAPA Biosystem's library preparation kit on the Illumina HiSeq 2500 platform. Nimblegen SeqCap EZ version 3.0 rapid or Nimblegen SeqCap EZ version 4 was used for capture. Bioinformatic processing was performed by the Institute for Genomic Medicine's bioinformatic and trio analysis platforms using BWA and GATK, which identified qualifying genotypes after accounting for the parental genotypes and genotypes present in in-house and external control reference samples. Variants with a minor allele frequency (MAF) > 0.01 were excluded, and variants that were predicted pathogenic by American College of Medical Genetics (ACMG) guidelines were prioritized.[13] The *TMEM218* variants were validated by Sanger sequencing.

RUMC family: After a gene panel analysis for vision disorders failed to identify biallelic RDVs, clinical exome sequencing revealed the *TMEM218* variants reported in this work. In brief, exome sequencing was performed using an Illumina HiSeq system and Agilent SureSelectXT Human All exome 50 Mb kit. Following read alignment (BWA) and variant calling via GATK (single nucleotide variant, SNV) and CoNIFER (copy number variant, CNV), variants were annotated using an in-house developed pipeline. Variants with a MAF above 5% in Single Nucleotide Polymorphism Database (dbSNP) and above 1% in an in-house database were excluded. ACMG 2015 guidelines were used as criteria for variant pathogenicity.[13]

UCL family: Exome sequencing was performed on DNA as previously described.[14] Based on the presence of consanguinity and a ciliopathy-related phenotype, we prioritized recessive homozygous coding variants within runs of homozygosity. We excluded synonymous variants, intronic variants (>5 bp from exon boundaries) and common variants (MAF, >0.001% via population databases). Variants that were predicted pathogenic by Sorting Intolerant From Tolerant (SIFT),[15] Polymorphism Phenotyping v2 (PolyPhen2),[16] and MutationTaster[17] were prioritized. The *TMEM218* variants were validated by Sanger sequencing.

AUMC family: After clinical exome sequencing with a ciliopathy panel of 142 genes failed to identify biallelic RDVs, clinical exome sequencing identified the pathogenic *TMEM218* variants reported here. In brief, DNA was extracted from peripheral blood samples and enriched with the Agilent SureSelectXT Human All Exon 50 Mb Kit (Santa Clara, CA, USA). Exome sequencing was performed using an Illumina NextSeq500 (San Diego, CA, USA). Following read alignment with BWA and variant calling with GATK, variants were annotated using an in-house developed program at the department of Genetics of the Radboud University Medical Center. ACMG 2015 guidelines were used as criteria for variant pathogenicity.[13] In brief, data on frequency of variants in control populations (<5% in dbSNP and <1% in an in-house database), nucleotide and amino acid conservation, inheritance pattern, and the phenotype associated with the genes were combined to prioritize variants. All reported variants that did not meet our validated quality standard were confirmed using Sanger sequencing.

Results

TMEM218 variants cause JBTS

To identify novel genes associated with JBTS, we performed exome sequencing on 53 individuals from a cohort of 655 families affected by JBTS, in whom we did not identify pathogenic variants in candidate or known genes associated with the disorder.[4] We identified a single individual (UW362-4) with biallelic RDVs, affecting the same

amino acid residue (g.124967611C>T [NC_000011.9] [c.344G>A (GenBank: Se_001258243.1); p.Arg115His (NP_001245172.1)] maternal and g.124967612G>A [GenBank: NC_000011.9] [c.343C>T (NM_001258243.1); p.Arg115Cys (GenBank: NP_001245172.1)] paternal), which are rare in gnomAD v2.1[18,19] and predicted to be deleterious by the CADD algorithm (Figure 1; Table 1).[11] The affected fetal sibling (UW362-3) also carried these variants. We did not identify biallelic RDVs in other genes associated with the primary cilium. We then screened our cohort (i.e., 62 individuals with JBTS who had not been sequenced and 229 individuals with JBTS who had been previously sequenced but whose genetic etiology was unknown) using small molecule molecular inversion probes capture[4,9,20] and identifiedg.124967612G>A (GenBank: NC_000011.9) (c.343C>T [GenBank: NM_001258243.1];p.Arg115Cys [GenBank: NP_001245172.1]) homozygous in a fetus diagnosed with Meckel syndrome (UW363-3) (Figure 1; Table 1). Using the MyGene2 and GeneMatcher[21] nodes of MatchMaker Exchange,[22] we identified four additional families with *TMEM218* variants, all detected by exome sequencing: (1) CUMC family: homozygousc.343C>T (GenBank: NM_001258243.1) (p.Arg115Cys [GenBank: NP_001245172.1]) variant in three fetuses with occipital encephaloceles from Irish parents without known consanguinity (Figure 1; Table 1). This couple also had a previous pregnancy with ultrasound findings suspicious for lower urinary tract obstruction at 12 weeks gestation, followed by miscarriage at 14 weeks. (2) RUMC family: homozygous g.124967611C>T (GenBank: NC_000011.9) (c.344G>A [GenBank: NM_001258243.1];p.Arg115His [GenBank: NP_001245172.1]) variant in two adult siblings with developmental disability and retinal dystrophy from consanguineous Iraqi parents (Figure 1; Table 1). (3) UCL family homozygousg.124972112C>A (GenBank: NC_000011.9) (c.131G>T [GenBank: NM_001258243.1];p.Gly44Val [GenBank: NP_001245172.1]) variant in a female child with the molar tooth sign on brain MRI from consanguineous Irani parents (Figure 1; Table 1). (4) AUMC family: homozygousg.124971135G>A (GenBank: NC_000011.9) (c.280C>T [GenBank: NM_001258243.1];p.Arg94* [GenBank: NP_001245172.1]) variant in a fetus with encephalocele, polycystic kidneys, polydactyly, and hypoplastic left heart syndrome from consanguineous Pakistani parents (Figure 1; Table 1). Biallelic RDVs were not found in other compelling candidate genes in these families. Our best estimate is that TMEM218 dysfunction accounts for 0.16% of JS, based on identifying biallelic *TMEM218* variants in 1 out of 625 families in our cohort (105 directly sequenced and 420 with other well-established causes).

Bioinformatic tools, such as the HOPE (Have [y]our Protein Explained) resource,[23] predict that the missense variants reported in this work disrupt protein function. Both residues at position 44 and 115 are in conserved positions in or adjacent to transmembrane alpha helices, but not at predicted phosphosites.[24] Using Aminode, we found that resides 44 and 115 are in highly conserved and evolutionarily constrained regions (ECRs) across orthologs (Figure 1A).[25] Aminode identifies sites within proteins under evolutionary constraint. Local minima in the relative substitution score define these evolutionarily constrained regions, which indicate protein segments that are less tolerant to substitutions and enriched for pathogenic variants.

Phenotypic features associated with TMEM218 dysfunction

The classic molar tooth sign was demonstrated in the two individuals (UW362-4 and UCL-1) for whom postnatal brain imaging was available (Figures 2A and 2D). Vermis hypoplasia, a likely molar tooth sign, and brainstem dysplasia were demonstrated by fetal MRI in UW362-3 (Figures 2G–2I). Occipital encephalocele was identified by prenatal ultrasound in five fetuses from three families (Figures 2J and 2K). No other brain malformations were demonstrated.

The four living individuals (UW362-4, RUMC-1, RUMC-2, and UCL-1) have a range of developmental disability, from full dependence for all activities of daily living (ADLs) and non-verbal communication in UCL-1, to requiring some support for most ADLs and single words in UW362-4, to near independence for ADLs and simple sentence verbal communication in the RUMC siblings. All four individuals also have retinal dystrophy (from Leber congenital amaurosis to early-onset rod-cone retinal dystrophy), but no known kidney or liver involvement (Table 1). Two fetuses (UW363-3 and AUMC-1) had polydactyly and polycystic kidneys in addition to occipital encephalocele, warranting a Meckel syndrome diagnosis (Table 1). AUMC-1 also had hypoplastic left heart syndrome, characterized by absent mitral valve, small left ventricle, large ventriculoseptal defect, cardiomegaly, and mild pericardial effusion. (Figures 2N and 2O; Table 1). Additional features may have been missed in the fetuses due to early gestational age (11–12 weeks) at imaging and/or lack of autopsy.

Discussion

Here we present evidence for TMEM218 dysfunction causing ciliopathies along the Joubert-Meckel syndrome spectrum. We identified biallelic RDVs in ten individuals from six families. The four living affected individuals (UW362-4, RUMC-1, RUMC-2, and UCL-1) have developmental disability with retinal dystrophy, likely representing the milder end of the Joubert-Meckel spectrum. The fetal sibling of UW362-4 (UW362-3) did not display any additional features at time of demise. The three fetal siblings (CUMC-1, CUMC-2, and CUMC-3) likely represent the severe end of JBTS, as they had occipital encephaloceles identified very early in gestation. The two other fetuses (UW363-3 and AUMC-1) had features consistent with Meckel syndrome: occipital encephalocele,

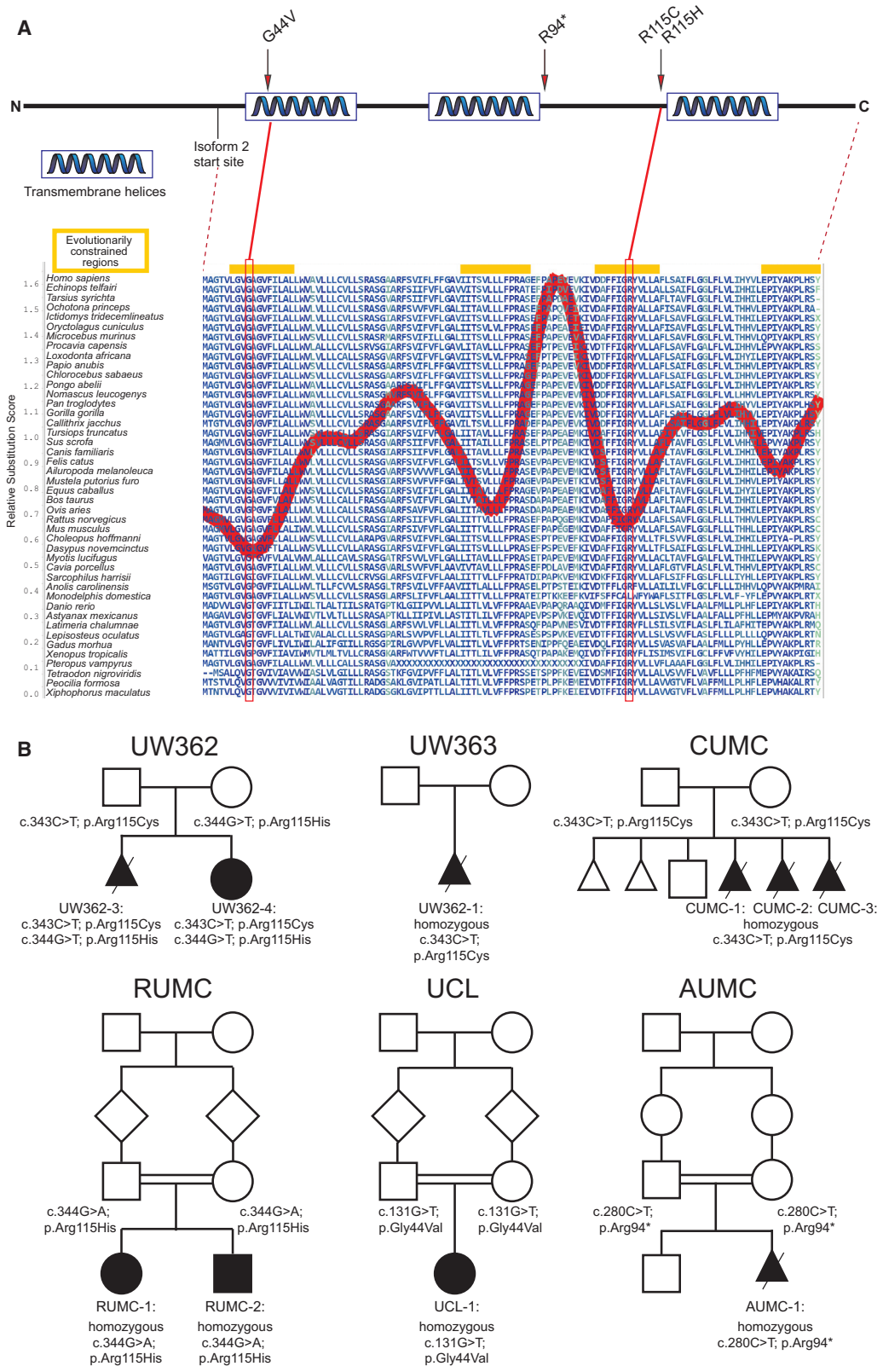

Figure 1. ***TMEM218*** **variants cause ciliopathy phenotypes**
(A) The *TMEM218* gene encodes a protein with three transmembrane helices. Individual variants are indicated by red arrows. The two highly conserved missense variants are in the most evolutionarily constrained regions that are intolerant to substitutions.
(B) Pedigrees are consistent with recessive inheritance. The affected individual and fetuses are indicated with filled black shapes.

Table 1. Clinical features associated with biallelic, pathogenic *TMEM218* variants

ID#	Variants	AF	CADD	Ethnicity	Sex	Age	Developmental disability	Brain	Retinal dystrophy	Kidney	PD	Other
UW362-3	c.344G>A; p.Arg115His mat	0.00001596	27.9	European/ North Indian	M	N/A	N/A	VH	N/A	N	N	pregnancy terminated, posterior fossa cyst on autopsy
UW362-4	c.343C>T; p.Arg115Cys pat	0.00004986	35		F	15 years	Y	MTS	Y[a]	N	N	apnea/tachypnea, abnormal eye movements, congenital left Erb palsy, high pain tolerance, sensitive to temperature changes
UW363-3 / GM07817	c.343C>T; p.Arg115Cys hmz	0.00004986	35	African American	F	N/A	N/A	OE	N/A	Y[a]	Y	pregnancy terminated, contractures
CUMC-1	c.343C>T; p.Arg115Cys hmz	0.00004986	35	Irish	M	12 weeks	N/A	OE	N/A	N/A	N/A	pregnancy terminated
CUMC-2					F	11 weeks	N/A	OE	N/A	N/A	N/A	pregnancy terminated
CUMC-3					M	12 weeks	N/A	OE	N/A	N/A	N/A	pregnancy terminated
RUMC-1	c.344G>A; p.Arg115His hmz	0.00001596	27.9	Iraqi	F	25 years	Y	N/A	Y	N	N	overweight, 5th finger camptodactyly
RUMC-2					M	19 years	Y	N/A	Y	N	N	overweight, 5th finger camptodactyly, micro-orchidism, mild ptosis
UCL-1	c.131G>T: p.Gly44Val hmz	0	26.9	Irani	F	5 years	Y	MTS	LCA	N	N	ocular motor apraxia, severe speech disorder
AUMC-1	c.280C>T; p.Arg94* hmz	0.00002396	40	Pakistani	M	19+ 5/7 weeks	N/A	OE	N/A	Y[b]	Y	pregnancy terminated, hypoplastic left heart syndrome

Abbreviations: AF, allele frequency in gnomAD[18,19]; CADD, Combined Annotation Dependent Depletion v1.3 score[11]; F, female; hmz, homozygous; LCA, Leber congenital amaurosis; M, male; mat, maternal; MTS, molar tooth sign; N, no; N/A, not available; OE, occipital encephalocele; pat, paternal; PD, polydactyly; unk, unknown; VH, cerebellar vermis hypoplasia; Y, yes. GenBank: NM_001258243.1.
[a]Rod-cone dystrophy, onset < 1 year.
[b]Polycystic kidneys by ultrasound.

polydactyly, and polycystic kidneys. Remarkably, four of these families share the p.Arg115Cys variant. Given their ethnic backgrounds and the presence of p.Arg115Cys in Northwestern European (12/50,514), Other non-Finnish European (1/32,924), and South Asian (1/30,158) individuals in gnomAD,[19] we cannot conclusively determine whether p.Arg115Cys represents a founder variant or results from a mutational hotspot.

Predicted variant severity may correlate with phenotypic severity. The homozygous nonsense variant p.Arg94* in AUMC-1 is predicted to be the most deleterious to protein function and is associated with the most severe phenotype with encephalocele, polydactyly, cystic kidneys, and hypoplastic left heart. This early stop codon is likely to result in nonsense-mediated decay. The missense variant p.Arg115Cys may be more disruptive to protein function than the other missense variants, since all fetuses with this homozygous variant had encephaloceles detected early in gestation. Variants p.Arg115His and p.Gly44Val may be less disruptive, since individuals with these variants are capable of living into adulthood. Indeed, the CADD algorithm also ranks the variants accordingly: p.Arg94*(40) > p.Arg115Cys(35) > p.Arg115His(27.9) > p.Gly44Val(26.9). Additional individuals and/or functional work would be needed to test this allelic series more thoroughly.

So far, all living individuals with pathogenic *TMEM218* variants have developed retinal dystrophy, and half of the affected fetuses had cystic kidney disease. This may indicate a higher risk for these features than individuals

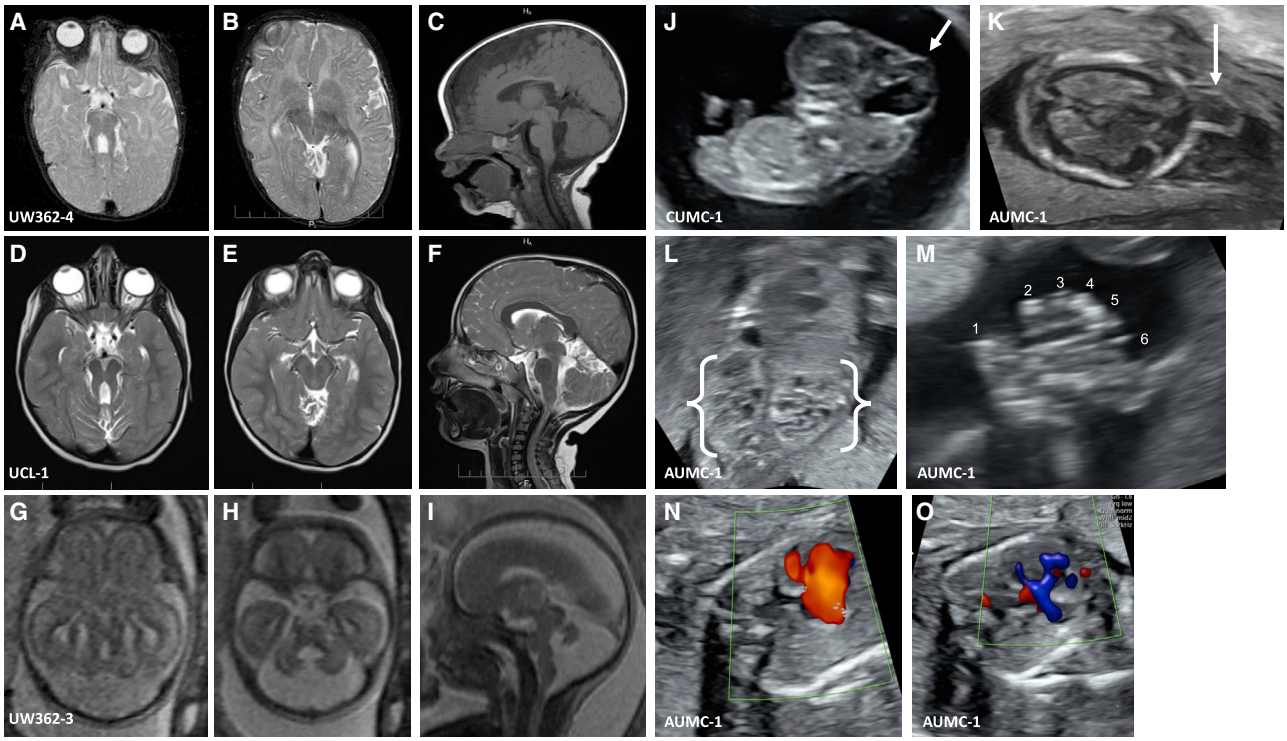

Figure 2. Imaging features associated with TMEM218-related Joubert and Meckel syndromes
(A–F) Post-natal brain MRI showing classic molar tooth sign (A and D), superior cerebellar dysplasia (B and E), and elevated roof of the fourth ventricle (C and F) in UW362-4 (A–C) and UCL-1 (D–F).
(G–I) Fetal MRI showing likely molar tooth sign (G), cerebellar vermis hypoplasia (H), and elevated roof of the fourth ventricle (I) in UW362-3.
(J and K) Prenatal ultrasound showing occipital encephalocele in CUMC-1 at 12 weeks gestation and AUMC-1 at 14 weeks gestation (arrows).
(L and M) Prenatal ultrasound showing large, cystic kidneys (brackets) and post-axial hand polydactyly (numbers) in AUMC-1 at 14 weeks gestation.
(N and O) Fetal echocardiogram showing diastolic filling of the left ventricle only from the right ventricle via a ventriculoseptal defect (red in N) and systolic filling of the great vessels predominantly from the right ventricle (blue in O) tracks in AUMC-1 at 18 weeks gestation.

with other causes of JBTS, so they should be monitored closely with baseline kidney ultrasound, serial laboratory testing (creatinine and/or cystatin C, and hemoglobin), and serial ophthalmology evaluations, ideally with optical coherence tomography.[3] Liver involvement was not reported, so we recommend standard monitoring for portal hypertension (due to liver fibrosis) by serum platelet levels and ultrasound measurement of spleen size every 1–2 years. The presence of hypoplastic left heart syndrome in one fetus may indicate an increased risk for congenital heart defects, which should prompt a low threshold for echocardiogram, particularly if adequate cardiac views were not obtained by prenatal ultrasound. Heart defects are rare in JBTS[4,26] and inconsistently documented in Meckel syndrome,[27] but cilia have been widely implicated in congenital heart disease.[28] Additionally, the identification of a molecular genetic diagnosis allows families accurate reproductive genetic counseling with options, such as *in vitro* fertilization with preimplantation genetic diagnosis, use of a gamete donor, prenatal diagnosis via chorionic villus sampling or amniocentesis, and/or expectant management.

The primary cilium is a singular organelle that senses a wide range of chemical, light, and mechanical cues. It is found on nearly every type of human cell, offering some insight to the pleiotropic manifestations of ciliopathies. The basal body (BB), a modified centriole, docks at the apical plasma membrane and is the template for the ciliary core structure, the microtubule-based axoneme. As the doublet microtubules project upward for several microns, the transition zone (TZ) forms at the BB-axoneme interface and tethers the distal BB to the plasma membrane. Here the TZ partitions the cilium from the cytoplasm by regulating ciliary protein content and serving as a bi-directional diffusion barrier. The JBTS-associated proteins localize to multiple subregions of the cilium, but the TZ is a hotspot for ciliopathy-related proteins, and indeed, half of the JS-associated proteins localize to the region.

TMEM218 was recently identified as a TZ component based on endogenous tagging experiments in *C. elegans*.[8] Through a series of genetic interaction assays, Li et al.[8] found TMEM218 interacts with other TZ components in a module at the TZ periphery. Recent advances in super resolution microscopy have revealed details of TZ

organization. The dense TZ protein network is organized into concentric ring structures and can be functionally separated into modules, although we are just beginning to appreciate the plasticity of this region.[8,29–31] At the core of the TZ, JS-associated proteins RPGRIP1L, CEP290, and CC2D2A facilitate localization of other TZ components. NPHP1 and NPHP4 localize more peripherally. At the utmost periphery sits another distinct module, consisting of B9D1, B9D2, and several transmembrane proteins, including TMEM218 (also TMEM216, TMEM231, TMEM80, TMEM17, and TMEM237).[8] It is enticing to speculate that TMEM218 could be part of the ciliary necklace, a series of 3 rows of particles that encircle the cilium near the base, first observed by freeze-etch scanning electron microscopy of cilia in the mid-20th century.[32] Given its role in ciliary biology and association with so many ciliopathy-related proteins, Li et al.[8] also predicted that deleterious variants in this gene would cause ciliopathies. At the time, they sequenced an Italian JS cohort of 330 individuals with JS and did not find any likely pathogenic variants.[8] This is in line with our observations that *TMEM218* variants are a rare cause of JS.

At the organismal level, *Tmem218*$^{-/-}$ mice display progressive retinal degeneration and cystic kidney disease but not a brain phenotype observable by histology.[7] Subtle thinning of the outer segment layer in the retina was reported as early as 14 weeks of age, progressing to a pronounced stage of degeneration of both outer nuclear layer and photoreceptor inner and outer segments by 29 weeks. The cystic lesions displayed tubular atrophy, disrupted tubular basement membranes, and inflammatory cellular infiltrates and fibrosis of the renal tubulointerstitium. The combination of retina and kidney involvement led authors to postulate that TMEM218 dysfunction could cause Senior-Løken syndrome, another ciliopathy defined by these features, in humans.

Our data provide strong evidence that TMEM218 dysfunction results in ciliopathy phenotypes along the JBTS-Meckel spectrum. This finding is supported by functional work localizing TMEM218 to the ciliary TZ and a mouse model recapitulating the retinal and kidney phenotypes. Identifying the complete genetic and phenotypic spectrum of these ciliopathies directly improves diagnostic testing, guides medical surveillance, and allows for earlier treatment of complications. In addition, defining the molecular mechanisms underlying ciliopathies will serve as the basis for developing precision treatments in the future. This potential is already being realized with gene-specific therapies for retinal disease.[33] More broadly, given the key roles for cilia in development and mature organ function, understanding cilium function and dysfunction is likely to have important impacts on a diverse array of human conditions.

Data and code availability

The UW exome data will be available through dbGaP (dbGaP: phs000693). The clinical exomes are not publicly available. The variants generated during this study are available at ClinVar (Gene variants; ClinVar: SUB8476323).

Consortia

Michael J. Bamshad, Suzanne M. Leal, and Deborah A. Nickerson, Peter Anderson, Tamara J. Bacus, Elizabeth E. Blue, Kati J. Buckingham, Jessica X. Chong, Diana Cornejo Sánchez, Colleen P. Davis, Christian D. Frazar, Danielle Giroux, William W. Gordon, Martha Horike-Pyne, Jameson R. Hurless, Gail P. Jarvik, Eric Johanson, J. Thomas Kolar, Melissa P. MacMillan, Colby T. Marvin, Sean McGee, Daniel J. McGoldrick, Betselote Mekonnen, Patrick M. Nielsen, Karynne Patterson, Benjamin Pelle, Aparna Radhakrishnan, Matthew A. Richardson, Gwendolin T. Roote, Erica L. Ryke, Isabelle Schrauwen, Kathryn M. Shively, Joshua D. Smith, Monica Tackett, Machiko S. Threlkeld, Gao Wang, Jeffrey M. Weiss , Marsha M. Wheeler , Qian Yi, Jordan E. Zeiger, and Xiaohong Zhang.

Acknowledgments

We deeply thank the families who participated in this study. We also thank the Joubert syndrome and Related Disorder Foundation for referring families to the UW cohort. We would like to thank the contributors to MyGene2. This work was supported by the following: NIH Eunice Kennedy Shriver National Institute of Child Health and Human Development U54HD083091 (Genetics Core and Sub-project 6849) to D.D., NIH Eunice Kennedy Shriver National Institute of Child Health and Human Development 1K99HD100554-01 to J.C.V, NIH National Institute of Neurological Diseases and Stroke (R01NS064077 to D.D.), private donations from families to D.D., NIH National Human Genome Research Institute and National Heart, Lung, and Blood Institute (UM1 HG006493 and U24 HG008956) to M.J.B. and D.A.N., Columbia University internal funding to J.L.G., MRC Clinical Scientist fellowship (MR/K010654/1) to A.M.W., Paediatric Research award (Paed_RP_011_20170929) to A.M.W., Medical Research Council (MRC) (MR/S01165X/1 and MR/S005021/1) to R.M., The Wellcome Trust (Synaptopathies Strategic Award, WT093205MA and WT104033AIA) to R.M., and ongoing support from The Rosetree Trust, Ataxia UK, The MSA Trust, Brain Research UK, Sparks GOSH Charity, Muscular Dystrophy UK (MDUK), and Muscular Dystrophy Association (MDA USA) to R.M.

Declaration of interests

The authors declare no competing interests.

Received: August 5, 2020
Accepted: November 16, 2020

Web resources

Aminode, http://www.aminode.org
ClinVar, https://www.ncbi.nlm.nih.gov/clinvar/
Corielle Institute for Medical Research, https://www.coriell.org/
dbGaP, https://www.ncbi.nlm.nih.gov/gap/
Gene Matcher, https://genematcher.org

Mutation taster, http://www.mutationtaster.org/
MyGene2, https://mygene2.org/MyGene2/
OMIM, https://www.omim.org/
PolyPhen-2, http://genetics.bwh.harvard.edu/pph2/
SIFT, http://provean.jcvi.org/

References

1. Nuovo, S., Bacigalupo, I., Ginevrino, M., Battini, R., Bertini, E., Borgatti, R., Casella, A., Micalizzi, A., Nardella, M., Romaniello, R., et al. (2020). Age and sex prevalence estimate of Joubert syndrome in Italy. Neurology *94*, e797–e801.
2. Joubert, M., Eisenring, J.J., Robb, J.P., and Andermann, F. (1969). Familial agenesis of the cerebellar vermis. A syndrome of episodic hyperpnea, abnormal eye movements, ataxia, and retardation. Neurology *19*, 813–825.
3. Bachmann-Gagescu, R., Dempsey, J.C., Bulgheroni, S., Chen, M.L., D'Arrigo, S., Glass, I.A., Heller, T., Heon, E., Hildebrandt, F., Joshi, N., et al. (2020). Healthcare recommendations for Joubert syndrome. Am. J. Med. Genet. A. *182*, 229–249.
4. Bachmann-Gagescu, R., Dempsey, J.C., Phelps, I.G., O'Roak, B.J., Knutzen, D.M., Rue, T.C., Ishak, G.E., Isabella, C.R., Gorden, N., Adkins, J., et al. (2015). Joubert syndrome: a model for untangling recessive disorders with extreme genetic heterogeneity. J. Med. Genet. *52*, 514–522.
5. Shaheen, R., Szymanska, K., Basu, B., Patel, N., Ewida, N., Faqeih, E., Al Hashem, A., Derar, N., Alsharif, H., Aldahmesh, M.A., et al. (2016). Characterizing the morbid genome of ciliopathies. Genome Biol. *17*, 242.
6. Vilboux, T., Doherty, D.A., Glass, I.A., Parisi, M.A., Phelps, I.G., Cullinane, A.R., Zein, W., Brooks, B.P., Heller, T., Soldatos, A., et al. (2017). Molecular genetic findings and clinical correlations in 100 patients with Joubert syndrome and related disorders prospectively evaluated at a single center. Genet. Med. *19*, 875–882.
7. Vogel, P., Gelfman, C.M., Issa, T., Payne, B.J., Hansen, G.M., Read, R.W., Jones, C., Pitcher, M.R., Ding, Z.M., DaCosta, C.M., et al. (2015). Nephronophthisis and retinal degeneration in tmem218−/− mice: a novel mouse model for Senior-Loken syndrome? Vet. Pathol. *52*, 580–595.
8. Li, C., Jensen, V.L., Park, K., Kennedy, J., Garcia-Gonzalo, F.R., Romani, M., De Mori, R., Bruel, A.L., Gaillard, D., Doray, B., et al. (2016). MKS5 and CEP290 Dependent Assembly Pathway of the Ciliary Transition Zone. PLoS Biol. *14*, e1002416.
9. O'Roak, B.J., Vives, L., Fu, W., Egertson, J.D., Stanaway, I.B., Phelps, I.G., Carvill, G., Kumar, A., Lee, C., Ankenman, K., et al. (2012). Multiplex targeted sequencing identifies recurrently mutated genes in autism spectrum disorders. Science *338*, 1619–1622.
10. Chong, J.X., Buckingham, K.J., Jhangiani, S.N., Boehm, C., Sobreira, N., Smith, J.D., Harrell, T.M., McMillin, M.J., Wiszniewski, W., Gambin, T., et al. (2015). The Genetic Basis of Mendelian Phenotypes: Discoveries, Challenges, and Opportunities. Am. J. Hum. Genet. *97*, 199–215.
11. Rentzsch, P., Witten, D., Cooper, G.M., Shendure, J., and Kircher, M. (2019). CADD: predicting the deleteriousness of variants throughout the human genome. Nucleic Acids Res. *47*, D886–D894.
12. Petrovski, S., Aggarwal, V., Giordano, J.L., Stosic, M., Wou, K., Bier, L., Spiegel, E., Brennan, K., Stong, N., Jobanputra, V., et al. (2019). Whole-exome sequencing in the evaluation of fetal structural anomalies: a prospective cohort study. Lancet *393*, 758–767.
13. Richards, S., Aziz, N., Bale, S., Bick, D., Das, S., Gastier-Foster, J., Grody, W.W., Hegde, M., Lyon, E., Spector, E., et al. (2015). Standards and guidelines for the interpretation of sequence variants: a joint consensus recommendation of the American College of Medical Genetics and Genomics and the Association for Molecular Pathology. Genet. Med. *17*, 405–424.
14. Makrythanasis, P., Maroofian, R., Stray-Pedersen, A., Musaev, D., Zaki, M.S., Mahmoud, I.G., Selim, L., Elbadawy, A., Jhangiani, S.N., Coban Akdemir, Z.H., et al. (2018). Biallelic variants in KIF14 cause intellectual disability with microcephaly. Eur. J. Hum. Genet. *26*, 330–339.
15. Choi, Y., Sims, G.E., Murphy, S., Miller, J.R., and Chan, A.P. (2012). Predicting the functional effect of amino acid substitutions and indels. PLoS ONE *7*, e46688.
16. Adzhubei, I.A., Schmidt, S., Peshkin, L., Ramensky, V.E., Gerasimova, A., Bork, P., Kondrashov, A.S., and Sunyaev, S.R. (2010). A method and server for predicting damaging missense mutations. Nat. Methods *7*, 248–249.
17. Schwarz, J.M., Cooper, D.N., Schuelke, M., and Seelow, D. (2014). MutationTaster2: mutation prediction for the deep-sequencing age. Nat. Methods *11*, 361–362.
18. Lek, M., Karczewski, K.J., Minikel, E.V., Samocha, K.E., Banks, E., Fennell, T., O'Donnell-Luria, A.H., Ware, J.S., Hill, A.J., Cummings, B.B., et al. (2016). Analysis of protein-coding genetic variation in 60,706 humans. Nature *536*, 285–291.
19. Karczewski, K.J., Francioli, L.C., Tiao, G., Cummings, B.B., Alfoldi, J., Wang, Q., Collins, R.L., Laricchia, K.M., Ganna, A., Birnbaum, D.P., et al. (2020). The mutational constraint spectrum quantified from variation in 141,456 humans. Nature *581*, 434–443.
20. Hiatt, J.B., Pritchard, C.C., Salipante, S.J., O'Roak, B.J., and Shendure, J. (2013). Single molecule molecular inversion probes for targeted, high-accuracy detection of low-frequency variation. Genome Res. *23*, 843–854.
21. Sobreira, N., Schiettecatte, F., Valle, D., and Hamosh, A. (2015). GeneMatcher: a matching tool for connecting investigators with an interest in the same gene. Hum. Mutat. *36*, 928–930.
22. Philippakis, A.A., Azzariti, D.R., Beltran, S., Brookes, A.J., Brownstein, C.A., Brudno, M., Brunner, H.G., Buske, O.J., Carey, K., Doll, C., et al. (2015). The Matchmaker Exchange: a platform for rare disease gene discovery. Hum. Mutat. *36*, 915–921.
23. Venselaar, H., Te Beek, T.A., Kuipers, R.K., Hekkelman, M.L., and Vriend, G. (2010). Protein structure analysis of mutations causing inheritable diseases. An e-Science approach with life scientist friendly interfaces. BMC Bioinformatics *11*, 548.
24. Blom, N., Gammeltoft, S., and Brunak, S. (1999). Sequence and structure-based prediction of eukaryotic protein phosphorylation sites. J. Mol. Biol. *294*, 1351–1362.
25. Chang, K.T., Guo, J., di Ronza, A., and Sardiello, M. (2018). Aminode: Identification of Evolutionary Constraints in the Human Proteome. Sci. Rep. *8*, 1357.
26. Karp, N., Grosse-Wortmann, L., and Bowdin, S. (2012). Severe aortic stenosis, bicuspid aortic valve and atrial septal defect in a child with Joubert Syndrome and Related Disorders (JSRD) - a case report and review of congenital heart defects reported in the human ciliopathies. Eur. J. Med. Genet. *55*, 605–610.

27. Hartill, V., Szymanska, K., Sharif, S.M., Wheway, G., and Johnson, C.A. (2017). Meckel-Gruber Syndrome: An Update on Diagnosis, Clinical Management, and Research Advances. Front Pediatr. *5*, 244.
28. Li, Y., Klena, N.T., Gabriel, G.C., Liu, X., Kim, A.J., Lemke, K., Chen, Y., Chatterjee, B., Devine, W., Damerla, R.R., et al. (2015). Global genetic analysis in mice unveils central role for cilia in congenital heart disease. Nature *521*, 520–524.
29. Yang, T.T., Su, J., Wang, W.J., Craige, B., Witman, G.B., Tsou, M.F., and Liao, J.C. (2015). Superresolution Pattern Recognition Reveals the Architectural Map of the Ciliary Transition Zone. Sci. Rep. *5*, 14096.
30. Shi, X., Garcia Iii, G., Van De Weghe, J.C., McGorty, R., Pazour, G.J., Doherty, D., Huang, B., and Reiter, J.F. (2017). Super-resolution microscopy reveals that disruption of ciliary transition-zone architecture causes Joubert syndrome. Nat. Cell Biol. *19*, 1178–1188.
31. Akella, J.S., Silva, M., Morsci, N.S., Nguyen, K.C., Rice, W.J., Hall, D.H., and Barr, M.M. (2019). Cell type-specific structural plasticity of the ciliary transition zone in C. elegans. Biol. Cell *111*, 95–107.
32. Gilula, N.B., and Satir, P. (1972). The ciliary necklace. A ciliary membrane specialization. J. Cell Biol. *53*, 494–509.
33. Cideciyan, A.V., Jacobson, S.G., Drack, A.V., Ho, A.C., Charng, J., Garafalo, A.V., Roman, A.J., Sumaroka, A., Han, I.C., Hochstedler, M.D., et al. (2019). Effect of an intravitreal antisense oligonucleotide on vision in Leber congenital amaurosis due to a photoreceptor cilium defect. Nat. Med. *25*, 225–228.